External Heat-Transfer Distribution on Film Cooled Turbine Vanes

RICHARD D. LANDER,* ROBERT W. FISH,† AND MIKIO SUO‡
United Aircraft Corporation, East Hartford, Conn.

Experiments were performed to determine the heat transfer to the suction surface of two film cooled first stage turbine vanes using two-row discrete hole cooling. Evaluation of the heat transfer to the film cooled vanes was made in a turbulent environment downstream of an aircraft turbojet engine combustor at moderately high primary gas stream temperatures and pressures. Results of these experiments provided quantitative data on the adiabatic film effectiveness for a number of blowing rates, and show decreased effectiveness levels when compared to measured values for a continuous slot in a wind tunnel environment. In addition the external heat transfer coefficients were obtained based on the difference between the film cooled adiabatic wall temperature and the wall temperature. The presence of film cooling holes increased the heat-transfer coefficients even without blowing. Further increases in the heat-transfer coefficients were measured in the presence of blowing with the largest increases in the region nearest the ejection.

Introduction

MODERN gas turbine engines, which use higher turbine inlet temperatures to achieve new levels of efficiency and power, utilize various techniques to cool the turbine vanes and blades subjected to these adverse thermal environments. Recent experience has demonstrated that film cooling is an effective means for maintaining acceptable airfoil metal temperatures and providing prolonged turbine life. Film cooling of turbine vanes and blades utilizes relatively cold compressor bleed air which is bypassed around the combustor and is ejected through holes in the airfoil wall to cool the surfaces downstream. Frequently, film cooling is combined with internal convective cooling to provide a well-balanced, effective, and efficient cooling design.

To achieve maximum cycle benefits, the design of film cooled turbine airfoils can be accomplished only if the heat loads to these airfoils can be accurately predicted for the actual turbine environment. Previous investigators have considered the hypothesis that the heat transfer to a film cooled surface can be predicted by utilizing the heat-transfer coefficient of the surface without injection in conjunction with the difference between the adiabatic wall temperature with secondary injection and the actual wall temperature. Scesa's[1] measurements of the local isothermal heat transfer to a flat plate at large distances downstream of a slot with normal injection agreed quite favorably with predicted turbulent heat transfer for a solid wall when the thermal potential was based on the difference between the film cooled adiabatic wall temperature and the primary gas stream temperature. Similar results were obtained by Seban and Back[2] in the downstream region beyond the mixing zone for tangential injection on a flat plate while, in the mixing region, some dependence of the heat transfer on the slot velocity was noted. Further experimental verification that heat transfer far downstream of a tangential slot can be adequately predicted by the uncooled heat-transfer coefficient in combination with the previously described temperature difference was obtained by Hartnett et al.[3,4] At locations near the slot, however, significant increases in Stanton number were noted, especially for the higher blowing rates.

Metzger et al.[5] however, showed significant increases in heat-transfer coefficients on the film cooled surface up to 70 slot widths downstream of slots at an injection angle of 60° when the thermal driving potential was based on this same temperature difference.

Although most experimental investigations have dealt with heat-transfer and film effectiveness downstream of slots, a limited number of experimentors have evaluated the effects of injection from a single row of discrete holes. Metzger and Fletcher[6] considered injection through holes angled at 20° and 60° to the primary stream and discovered that these injection geometries gave poorer cooling protection than slots. In addition, Metzger found little difference in the heat-transfer coefficients between an uncooled wall and a wall with 20° angle holes but large increases near the holes with the 60° angle. Poorer cooling effectiveness for a single row of holes when compared to the continuous slot was also observed by Goldstein et al.[7]

Although these investigations have yielded significant insight into heat transfer in the presence of film cooling, consideration must be given to geometric and environmental conditions which are typical of high-temperature turbine airfoils. Structural limitations generally preclude using continuous slots. In addition, maintaining structural integrity by minimizing thermal gradients and keeping temperature levels below material limits frequently requires greater film coverage than can be obtained with a single row of holes, since placing the holes too close together results in interacting stress fields surrounding the holes which cause unacceptable stress concentrations. A solution to this problem has been found in the frequently used double row geometry similar to the one shown in Fig. 1. In this way, areawise film coverage of 100% can be provided without violating the previously mentioned limitations.

Heat transfer to the surface of an airfoil either with or without ejection is also affected by the turbulence generated

Presented as Paper 72-9 at the AIAA 10th Aerospace Sciences Meeting, San Diego, Calif., January 17–19 1972; submitted February 17, 1972; revision received June 23, 1972. The authors wish to acknowledge the support of their colleagues who contributed to this effort, and, in particular, to J. F. Muska for his assistance in performing the tests and L. L. Grimme for her help with the data reduction. In addition, portions of this study were supported by the U.S. Air Force Propulsion Laboratory, Air Force Systems Command, Wright-Patterson Air Force Base, Ohio, under Contract F33615-68-C-1644.

Index categories: Aircraft Power Plant design and Installation; Boundary Layers and Convective Heat Transfer—Turbulent; Nozzle and Channel Flow.

* Assistant Project Engineer, Engineering Department, Pratt & Whitney Aircraft Division.

† Project Engineer, Engineering Department, Pratt & Whitney Aircraft Division.

‡ Senior Project Engineer, Engineering Department, Pratt & Whitney Aircraft Division.

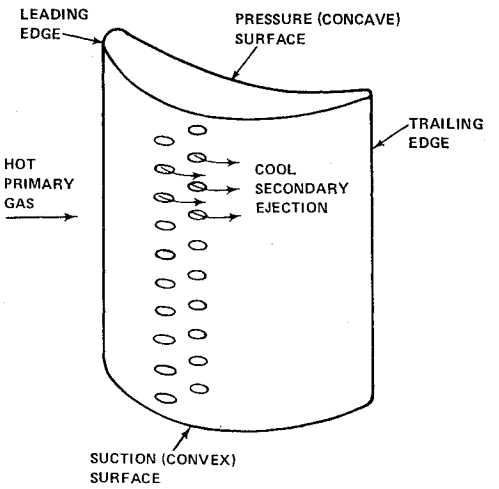

Fig. 1 Film cooled turbine airfoil.

in modern gas turbine engines. Significant decreases in film effectiveness were noted by Carlson and Talmore[8] when the turbulence of the freestream was increased from 3% to 22%. Although few measurements of combustor turbulence have been made in the adverse high temperature environment of a modern gas turbine, the work of Kuroch and Epik[9] indicates that turbulence levels are quite high. Quantitative evaluation of the effects of this freestream turbulence has yet to be made and previous wind-tunnel experiments have provided little simulation of the actual combustor turbulence.

To help alleviate the lack of film cooling information available for these types of injection geometries in combustor environments and to provide design criteria for predicting the film cooling effectiveness and the heat-transfer coefficients pertinent to realistic film cooled airfoils in the actual turbine environment, an experimental facility was set up which employed a shuttling cascade to determine airfoil heat transfer. This paper describes this test facility and presents typical results.

Test Apparatus

The experimental apparatus was constructed to enable determination of the adiabatic film effectiveness and the heat transfer rate to test airfoils employing discrete hole film cooling and to investigate heat-transfer characteristics in other cooled and noncooled turbine airfoils.

Measurements were made on instrumented test airfoils

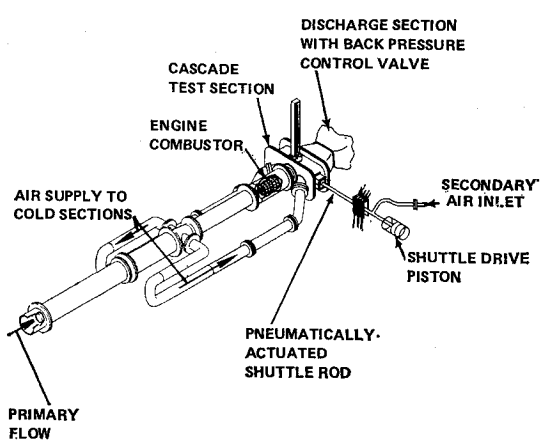

Fig. 2 Test apparatus.

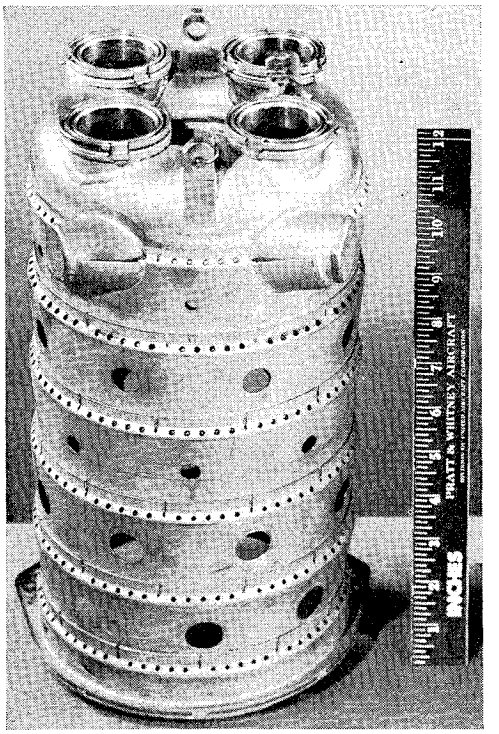

Fig. 3 Test rig combustor.

installed in four-passage cascades using 1) a steady-state mode of operation to measure the film effectiveness and 2) a transient mode to determine the heat-transfer rates. The test apparatus is shown in Fig. 2. It consisted basically of a gas turbine combustor which supplied hot exhaust to a three-airfoil test section. For the steady-state tests, the instrumented cascade was positioned in the high-temperature primary gas. In the transient tests, the cascade was shuttled rapidly between the bypass duct, where the air was at a relatively low temperature, and the hot primary gas.

During the tests, high pressure primary air was ducted into the test apparatus from a centrifugal compressor at a temperature of 100°F. Following metering of the primary flow with a standard VDI orifice, air was bled from this flow to provide cool bypass air. The remainder of the primary air continued through the ducting to a combustor located immediately upstream of the test section where the primary air temperature was raised to 600°F. The 7-in. diam combustor shown in Fig. 3 contained four fuel injection nozzles and, except for minimal alterations to adapt it for use in the test apparatus, is typical of those employed in many present day gas turbines. JP5 jet engine fuel was used in the combustor during the entire program.

Downstream of the combustor, a short transition duct is

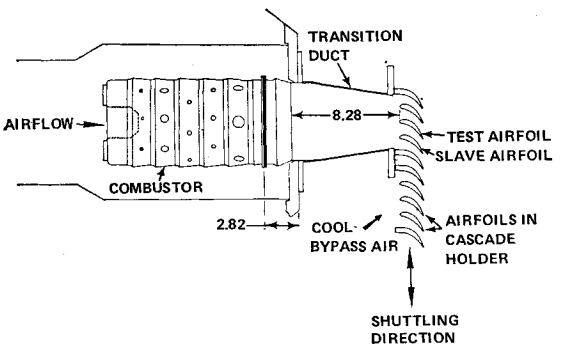

Fig. 4 Rig test section.

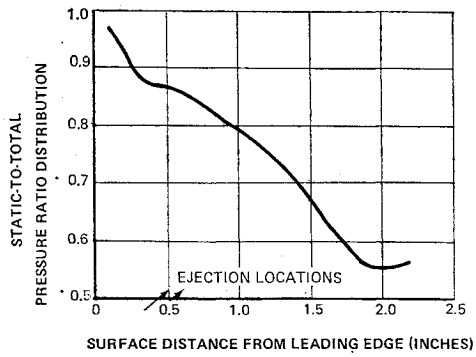

Fig. 5 Suction surface static-to-total pressure ratio distribution, airfoil 1.

utilized to mate with the inlet geometry of the cascade holder as shown in Fig. 4. The cascade holder was enclosed in the test section and the upstream face of the holder fitted flush with the downstream face of its transition duct with only a sliding fit permitted. The cascade holder was mounted on rollers to permit free and easy lateral movement. Rapid lateral shuttling of the cascade was performed with a large diameter pneumatically driven piston. This driving piston was located outside the test section and was connected to the cascade holder by a rod which also served as a conduit for the secondary film cooling air and the leads for the test airfoil instrumentation. The secondary air was supplied from a separate compressor source and entered the cascade holder rod at 100°F after being metered by a standard VDI orifice. Within the cascade holder, the secondary air to be used for film cooling was fed to the test airfoil through flexible tubing.

Downstream of the cascade was a large expansion duct whose exit flow area was controlled remotely with a butterfly valve, permitting back pressuring the system in order to set the cascade flow at the correct exit Mach number.

Since film cooling of two differently shaped turbine airfoils was investigated, two cascade holders were required. Each cascade holder contained two duplicate cascades of three airfoils and four passages adjacent to each other.

When operating the test apparatus in the transient mode, the primary gas flow conditions were set with the cascade containing the test airfoil in the cool by-pass air and the adjacent "dummy" cascade in the primary flow. Shuttling the instrumented cascade into the primary flow required approximately 0.050 sec, and except for a short time perturbation, little change in the primary flow was noted. Measurement of the heat-transfer rate was made shortly after the test airfoil was introduced into the hot primary flow and deviation of the test airfoil from the essentially isothermal state attained in the cool by-pass air was minimized.

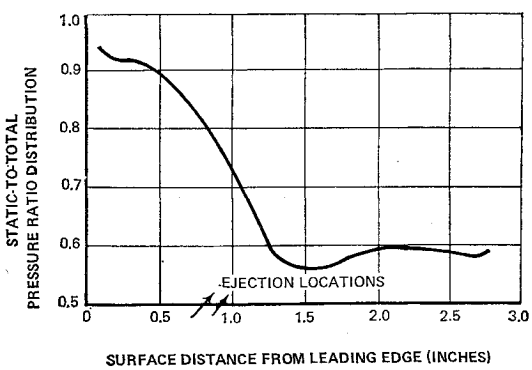

Fig. 6 Suction surface static-to-total pressure ratio distribution, airfoil 2.

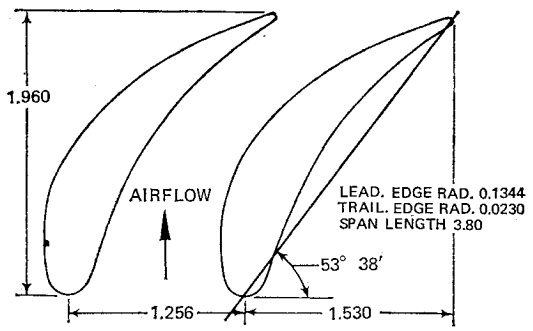

Fig. 7 Airfoil cross section, airfoil 1.

When running tests in the steady-state mode of operation, the instrumented airfoil remained in the hot primary flow stream and measurements were taken following attainment of equilibrium.

Test Airfoils

Two airfoil shapes containing different external static pressure distributions were studied. Both airfoils are typical of first stage vanes used in present day turbojet engines. Airfoil 1 is a high solidity subsonic vane and was tested in a two-dimensional plane cascade holder representative of the midspan section. Its suction surface external static-to-total pressure ratio distribution is shown in Fig. 5. Airfoil 2 was a low solidity subsonic vane and its midspan suction surface static-to-total pressure ratio distribution is shown in Fig. 6. The two airfoils are shown in cross section in Figs. 7 and 8.

Two methods of manufacturing the thin walled test airfoils were used to provide airfoils with the desired external contour. The first method, used for airfoil 1, was to cast the airfoil using an inner core to provide the cavity and thin wall. This method yielded a test airfoil with a nominal wall thickness of 0.048 in. and an excellent reproduction of the desired external contour but with small variations in the suction surface wall thickness. Airfoil 2 was made by forming nominal 0.030 in. thick sheet stock on an external mandrel to the desired airfoil shape. This latter method also provided excellent reproduction of the desired external contour in addition to a thinner wall, with little variation in wall thickness. Accurate measurements of the wall thickness at each thermocouple installation location were made for both test airfoils.

For the airfoils which were to be tested with film cooling, the inside cavity was partitioned to segregate the instrumented section from the coolant feed section. In all cases, the instrumented section was isolated into a "dead air space" to minimize forced convective losses from the back surface of the instrumented wall and to realize only the lower heat losses associated with free convection.

The 0.045-in. diameter film cooling holes were drilled into the suction surfaces of both airfoil shapes as indicated in Table 1. Locating the film cooling holes at a 2.78-in. diameter centerline-to-centerline spacing within each row provided 72% area-wise film coverage.

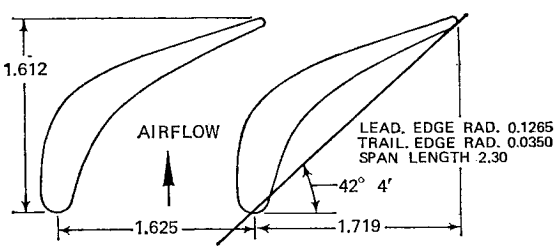

Fig. 8 Airfoil cross section, airfoil 2.

Table 1 Hole characteristics of test airfoils

	Airfoil 1		Airfoil 2	
	Upstream row	Downstream row	Upstream row	Downstream row
Angle of hole to the surface, deg	35	45	32	42
Leading-edge-to-hole surface distance, in.	0.484	0.584	0.796	0.921

Instrumentation

The inner suction surface of each test airfoil was instrumented at the midspan section with chromel-alumel thermocouples containing 0.003-in. diam leads. Each of the thermocouple wires was condenser welded to the surface approximately 0.005 in. apart to insure that the junction was in the wall of the test airfoil. Additional instrumentation was provided in the secondary film cooling passage to measure the coolant injection temperature. The primary gas stream total pressure and temperature were measured immediately upstream of the cascade. Thermocouple voltages were recorded on magnetic tape using a Transient Digital Data Acquisition System with "off line" computer conversion to engineering units. This system was designed to record large amounts of data during both transient and steady state operation of the test facility. In the tests with film cooling, it was possible to record the output from each thermocouple at intervals of approximately 0.005 sec, thus enabling a "continuous" time-wise measurement of the test airfoil's thermal response during transient operation.

Data Reduction

From the experiments, it was desired to obtain both the adiabatic film effectiveness and the heat transfer rate downstream of the film ejection locations. The adiabatic film effectiveness was defined as

$$\eta_f = (T_r - T_{aw})/(T_r - T_c) \tag{1}$$

where η_f = adiabatic film effectiveness; T_r = local primary gas adiabatic recovery temperature; T_{aw} = local adiabatic wall temperature with secondary ejection (commomly called the adiabatic film temperature); T_c = coolant temperature at ejection.

In expressing the heat transfer rate to the film cooled wall, the local external heat transfer coefficient, h_f, was used in conjunction with the difference between the adiabatic wall temperature and the actual wall temperature, i.e.,

$$h_f = q_c/(T_{aw} - T_{w_o}) \tag{2}$$

where q_c = heat convected to the wall from the primary stream per unit surface area; T_{w_o} = local wall external surface temperature.

When evaluating the test airfoils without blowing, the primary gas adiabatic recovery temperature was used as the driving potential. The heat-transfer rate was determined by performing a heat balance on the instrumented airfoil wall as shown schematically in Fig. 9 and algebraically in Eq. (3)

$$q_c + q_{ra} - q_k - q_{ci} - q_t = \rho l c_p(T_w) dT_w/d\tau \tag{3}$$

where: q_{ra} = net radiation to the surface per unit area
q_k = net lateral conduction within the wall per unit surface area
q_t = conduction through the thermocouple leads per unit surface area
q_{ci} = convection between the wall and inner air cavity per unit surface area
ρ = density of the wall element
T_w = average wall temperature
$c_p(T_w)$ = specific heat of wall element
l = thickness of instrumented wall
$dT_w/d\tau$ = time rate change of average wall temperature.

With the methods of airfoil construction and instrumentation employed, it was possible to neglect many of the terms in the heat balance when determining the external convective heat transfer rate. Radiation to the test airfoils from the surrounding vanes and ducting was estimated for the transient period and was found to be less than 1% of the external convective heat transfer. Conduction in the spanwise and chordal directions within the airfoil wall were also found to be negligible due to the thin wall of the test airfoil and very low thermal gradients in the spanwise and chordwise directions during the initial portion of the transient. In regions away from the thermocouples, the heat loss by free convection to the inner cavity was small.

The largest error in determining the external heat transfer was found to be heat conducted away from the area of the thermocouple junction through the chromel-alumel leads. In evaluating these losses, a three-dimensional finite element computer program for determining transient temperature distributions in irregularly shaped bodies was utilized. Results of this evaluation showed that, using the transient thermal response of the node simulating the thermocouple junction and assuming it to be indicative of the average metal temperature of the wall, yielded a result which differed from the actual external heat-transfer coefficient imposed upon the wall by approximately five percent. It should be noted that this error is in the absolute level of the external heat transfer coefficient. When heat-transfer coefficients are compared for various coolant flow rates, the thermocouple conduction errors would be similar provided heat-transfer rates were comparable in magnitude.

The heat balance was then simplified to

$$q_c = \rho l c_p(Tw) dT_w/d\tau \tag{4}$$

Using the definition of the external heat transfer coefficient and replacing T_{w_o} with T_w, Eq. (4) was written as

$$h_f = \rho l c_p(T_w) d(T_{aw} - T_w)/(T_{aw} - T_w) d\tau \tag{5}$$

or

$$h_f = -\rho l c_p[\ln(T_{aw} - T_{w2}) - \ln(T_{aw} - T_{w1})/(\tau_2 - \tau_1)] \tag{6}$$

where T_{w1} and T_{w2} are the wall temperatures at time τ_1 and τ_2, respectively.

Determination of the external heat transfer was made by evaluating the slope of a logarithmic representation of the difference between the adiabatic wall temperature and the actual wall temperature.

Measurement of the adiabatic wall temperature was made after equilibrium was reached with the film cooled test airfoil in the primary flow. Because of the thin wall, the low inner cavity heat-transfer coefficient and the linearity of the chordwise wall temperature distribution, the inside wall temperature was calculated to closely approximate the airfoil film temperature.

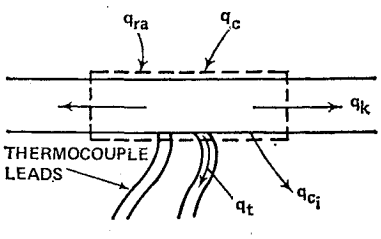

Fig. 9 Heat balance schematic.

Table 2 Primary gas stream test conditions

Nominal gas stream conditions		Axial chordal Reynolds number		Average exit Mach number	
Total temperature	Total pressure	Airfoil 1	Airfoil 2	Airfoil 1	Airfoil 2
600°F	40 psia	2.96×10^5	2.44×10^5	0.85	0.82
600°F	80 psia	5.92×10^5	4.87×10^5	0.85	0.82

The experimental uncertainties in the calculated adiabatic film effectiveness and the heat-transfer coefficients near the ejection holes due to expected random errors in the measured temperatures were determined by the methods of Kline and McClintock.[10] Results yielded uncertainties of $\pm 5\%$ in the calculated values of the film effectiveness and $\pm 8\%$ in the values of the heat-transfer coefficients with secondary ejection. Uncertainties in the calculated value of the heat-transfer coefficient without blowing were determined to be $\pm 3\%$.

Results and Discussion

Evaluation of the test airfoils was acomplished at the two primary gas stream conditions shown in Table 2. Both the adiabatic film effectiveness and the external heat-transfer coefficient were determined at the midspan section of the suction surface for these conditions and the results are presented and discussed in the following sections.

Adiabatic Film Effectiveness

The adiabatic film effectiveness for airfoil 1 at the lower axial chordal Reynolds number ($Re_c = 2.96 \times 10^5$) is shown in Fig. 10. These results are presented for various blowing parameters as a function of the distance downstream of the film ejection locations, normalized by the equivalent slot thickness S_{eq}, which was defined as the thickness of a slot equivalent in area to the total flow area of the film ejection holes. The blowing parameter M was calculated as the ratio of the secondary mass flux based on the total ejection area and total measured coolant flow to the primary stream mass flux at the ejection location. As expected, decreasing effectiveness levels were noted with increasing distances from the ejection holes. At surface locations near the holes, the effectiveness values maximized with increased blowing parameter while further downstream the effectiveness levels increased continuously with increasing blowing rates. This is shown more emphatically in Fig. 11 where the effectiveness values are plotted as a function of blowing parameter for various surface locations downstream of ejection. Maximum values of the film effectiveness occurred at a blowing parameter of approximately 0.6 at the thermocouple location nearest the ejection holes while further downstream the blowing parameter at which maximum effectiveness occurred was larger. At far downstream surface locations, the effectiveness was still not maximized even with blowing parameters above 1.0.

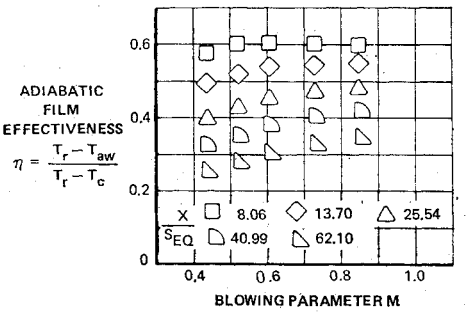

Fig. 11 Variation of film effectiveness with blowing for airfoil 1, $Re_c = 2.96 \times 10^5$.

The results at the high Reynolds number ($Re_c = 5.92 \times 10^5$) gas stream condition are presented in Fig. 12. Similar variations in film effectiveness values were noted as in the low Reynolds number environment. Comparison of the levels of effectiveness between the low and high Reynolds number gas stream conditions show almost identical results. Thus, doubling the Reynolds number had no apparent effect on the adiabatic film effectiveness of this test airfoil.

Since the length-to-diameter ratio of the film cooled holes was quite small, smoke tests were conducted in a free air environment to compare the angle of smoke ejection to the drilled angle of the holes. Results of these tests on airfoil 1 indicated the smoke ejection angle to be within five degrees of the drilled ejection angles.

It should also be noted that, as in most engine applications of double row discrete hole film cooling, both rows of suction surface secondary flow ejection holes were fed from the same coolant cavity and each row had approximately the same secondary flow driving pressure. Because of the slightly accelerating primary flow at the ejection locations (see Fig. 5) on the suction surface of airfoil 1, the downstream row of holes had a lower exit static pressure and thus a slightly greater portion of the total secondary fluid was ejected from this row. However, for airfoil 1 the pressure gradient was small in the region of ejection and each row of holes flowed close to the average of the two rows.

The adiabatic film effectiveness results for airfoil 2 at an axial chordal Reynolds number of 2.44×10^5, shown in Fig. 13, and the higher gas stream Reynolds number, shown in Fig. 14, depict similar trends as with airfoil 1. At the low Reynolds number maximizing of the film effectiveness near the holes occurred at blowing parameters slightly lower than 0.6 while further downstream the maximum occurrred at higher blowing rates. At the higher Reynolds number, however, maximum effectiveness was obtained at a blowing parameter of 0.5–0.6 even at large downstream distances. When comparison of the effectiveness levels of airfoil 1 and

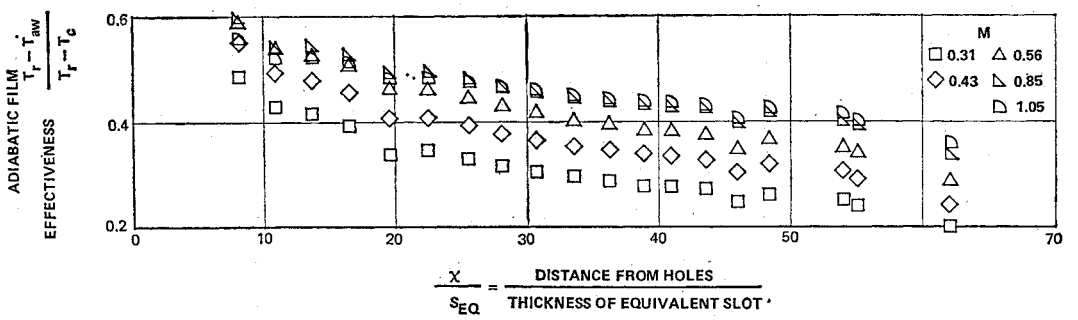

Fig. 10 Variation of film effectiveness with normalized chordal surface distance for airfoil 1, $Re_c = 2.96 \times 10^5$.

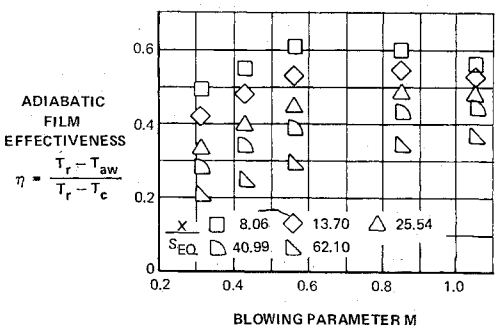

Fig. 12 Variation of film effectiveness with blowing for airfoil 1, $Re_c = 5.92 \times 10^5$.

airfoil 2 is made at the same distances from the holes and for similar blowing rates, it appears that film cooling on airfoil 2 was slightly less effective.

Measurement of the gas ejection angle with airfoil 2 in a free environment using smoke to compare the ejection angle to the drilling angle yielded larger deviations than airfoil 1 due to the smaller length-to-diameter ratio of the drilled ejection holes of airfoil 2. In general, the smoke ejection angles were approximately 27° further from the surface tangent than the drilled angles and, in part, might have contributed to the slightly lower levels of effectiveness.

Estimates were also made of the coolant flow splits for airfoil 2 and due to the significant acceleration of the primary stream in the area of the ejection, large differences in coolant flow were found between the rows. The results of these estimates for airfoil 2 are shown in Table 3.

The large differences in blowing parameters between the upstream and downstream rows could also be a reason for the lower effectiveness levels measured with airfoil 2. Because of these differences, it is difficult to discern whether the pressure distribution affected the film effectiveness levels.

The film effectiveness results for airfoil 1 are presented on an x/MS_{eq} basis in Fig. 15. Also shown are the results of

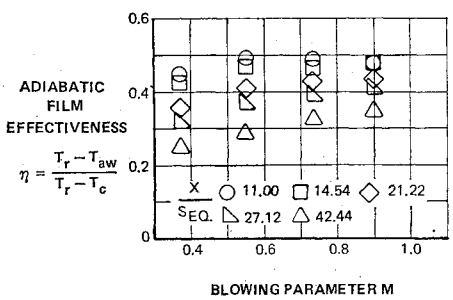

Fig. 13 Variation of film effectiveness with blowing for airfoil 2, $Re_c = 2.44 \times 10^5$.

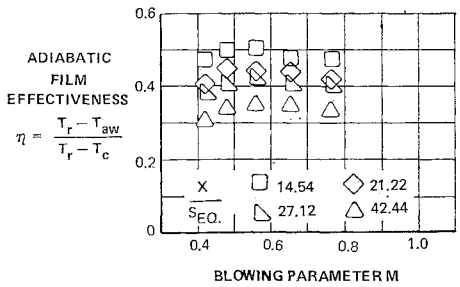

Fig. 14 Variation of film effectiveness with blowing for airfoil 2, $Re_c = 4.87 \times 10^5$.

Hartnett et al.,[3] obtained for a tangential slot in a low temperature wind tunnel environment, which indicate significantly higher levels of effectiveness than were obtained on the test airfoil. Also presented are the results of Metzger and Fletcher[6] obtained downstream of a single row of holes oriented at 60° to the surface with a 1.71 spacing-to-diameter ratio.

External Heat-Transfer Coefficients

The suction surface external heat-transfer coefficients on airfoil 1, based on the adiabatic wall temperature when secondary flow is ejected and on the adiabatic recovery temperature without ejection, were determined for the blank airfoil and for the drilled airfoil. A comparison of the heat transfer coefficients as a function of distance from the airfoil leading edge at a blowing parameter of 0.56 is shown in Fig. 16 for the low gas stream Reynolds number. Also shown are predictions of the heat transfer coefficients on the suction surface assuming laminar and turbulent flat plate boundary layers. The predictions utilize empirical results of cylinder-in-crossflow tests for the leading edge region.

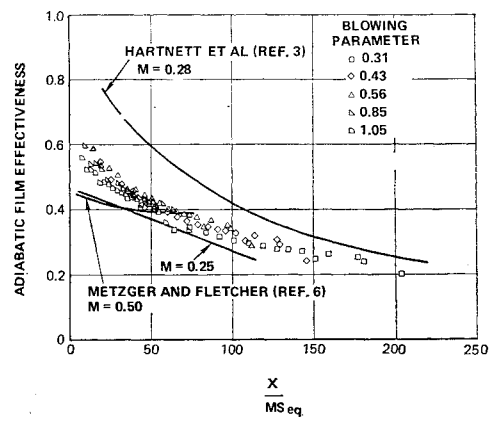

Fig. 15 Effectiveness of airfoil 1 on x/MS basis, $Re_c = 2.96 \times 10^5$.

Table 3 Coolant flow splits for airfoil 2

Gas stream Reynolds number	Over-all blowing parameter	Coolant flow split (percent of total)		Blowing parameter	
		Upstream row	Downstream row	Upstream row	Downstream row
2.44×10^5	0.38	32.0	68.0	0.26	0.48
	0.55	40.4	59.6	0.48	0.61
	0.73	43.9	56.1	0.69	0.76
	0.90	45.5	54.5	0.88	0.91
4.87×10^5	0.42	34.5	65.5	0.31	0.51
	0.48	37.7	62.3	0.39	0.50
	0.56	40.6	59.4	0.49	0.62
	0.66	42.7	57.3	0.60	0.70
	0.76	44.3	55.7	0.73	0.79

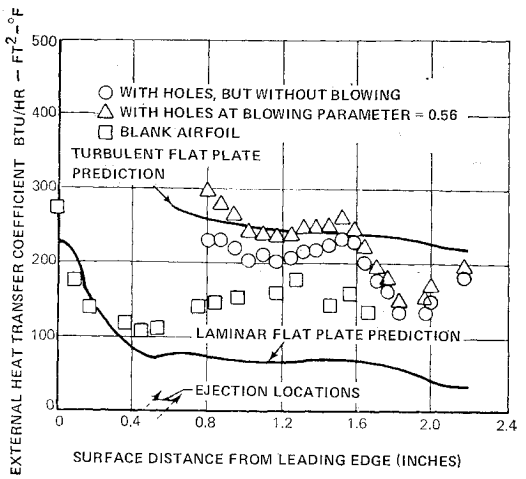

Fig. 16 Heat-transfer coefficients for airfoil 1 at $M = 0.56$, $Re_c = 2.96 \times 10^5$.

As shown in Fig. 16, the data for the blank airfoil indicates a laminar boundary layer in the upstream portion of the airfoil but showed increased heat transfer in the midchord region. Drilling the film cooling holes in the airfoil increased the heat-transfer coefficients downstream of the holes to values typical of a turbulent boundary layer. When the coolant was turned on, further increases in the heat-transfer coefficients were measured, with the greatest increases immediately downstream of the holes.

Similar results were obtained at the other blowing rates as shown in Fig. 17, which presents the ratio of the heat-transfer coefficients on the drilled airfoil in the presence of blowing to those measured with the secondary flow shut off. Large increases of over 30% were recorded near the holes with the amount of increase in the heat transfer coefficients being greatest for the highest blowing rates. Further downstream, however, the largest increases were obtained at the lower blowing rates.

The results of testing airfoil 1 in the high Reynolds number (Re-5.92 $\times$ 10^5) environment are shown in Fig. 18. Again, relatively large increases in heat transfer coefficients were measured near the holes with blowing. Increases of 50% over the nonblowing case were found near the hole pattern, decreasing to approximately 10% far downstream. As with the lower Reynolds number test, the greatest increases were found at the higher blowing rates near the holes and at the lower blowing rates further downstream.

For airfoil 2 the heat-transfer coefficients are presented for the case with no film cooling holes in the airfoil and for the case of secondary ejection. Because of the favorable pressure gradient in the area of the secondary ejection holes, aspiration into the upstream row of holes when the external coolant supply was shut off precluded presenting heat-transfer coefficients for this no blowing case. The results are shown in Figs. 19 and 20 for blowing rates of 0.55 and 0.56 at each of the two gas stream Reynolds numbers, respectively, together with the laminar and turbulent flat plate boundary layer predictions. For the blank airfoil, higher values of heat transfer than the laminar prediction were obtained at the lower Reynolds numbers in the upstream position of the airfoil. Further downstream, the data indicates transition has occurred, with the results agreeing fairly well with the turbulent boundary-layer prediction. When secondary flow was introduced, there were significant increases in the external heat-transfer coefficient near the holes, while downstream the values tended toward the level obtained near the trailing edge for the blank airfoil.

Conclusions

1) A cascade facility has been developed which permits evaluating the adiabatic film effectiveness and heat transfer to turbine airfoils employing practical secondary ejection configurations in a realistic turbine environment.

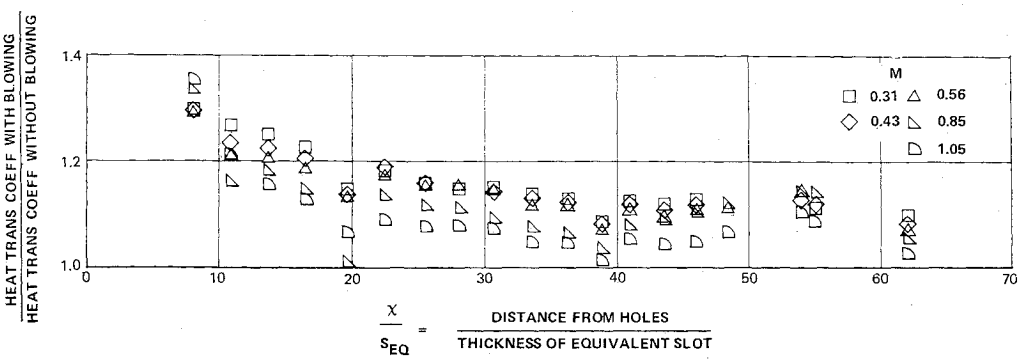

Fig. 17 Heat-transfer coefficient ratio for airfoil 1 at various blowing parameters, $Re_c = 2.96 \times 10^5$.

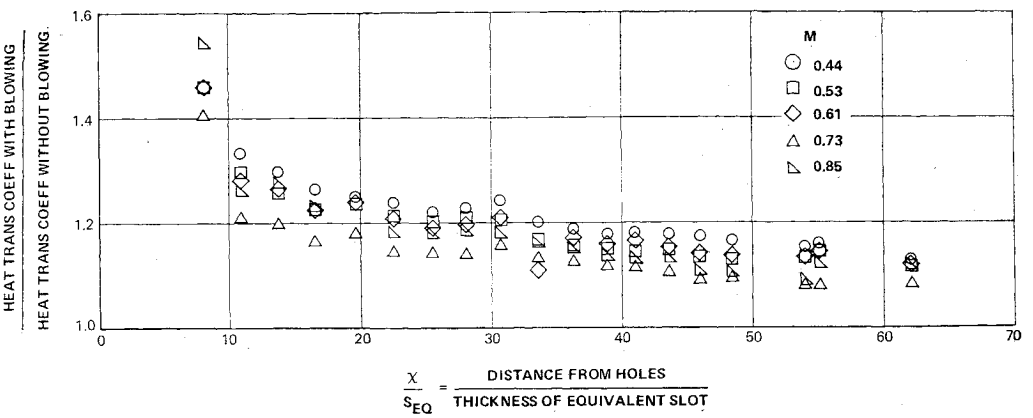

Fig. 18 Heat-transfer coefficient ratio for airfoil 1 at various blowing parameters, $Re_c = 5.92 \times 10^5$.

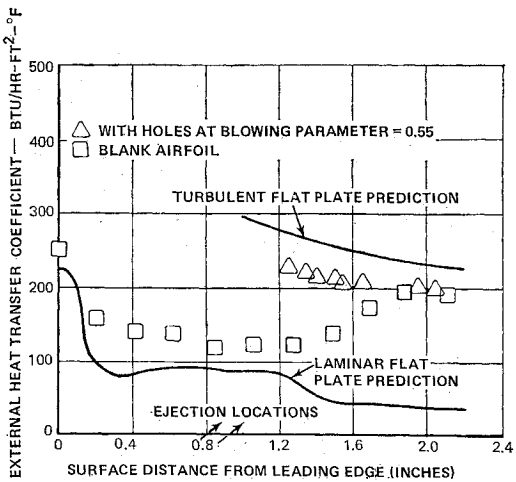

Fig. 19 Heat-transfer coefficients for airfoil 2 at $M = 0.55$, $Re_c = 2.44 \times 10^5$.

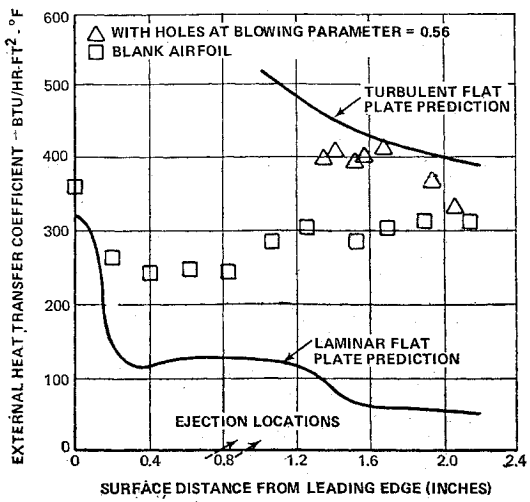

Fig. 20 Heat-transfer coefficients for airfoil 2 at $M = 0.56$, $Re_c = 4.87 \times 10^5$.

2) Film cooling on turbine airfoils with discrete hole ejection downstream of an engine type combustor yields film effectiveness levels significantly lower than those values obtained for slots in a wind tunnel environment, when compared at similar values of X/Ms_{eq}. Near the holes, highest effectiveness levels are obtained at blowing parameters of 0.5–0.6 while further downstream the levels generally increase with increasing blowing.

3) The presence of film cooling holes on turbine airfoils can increase the heat transfer even without blowing, while even higher heat-transfer coefficients can be expected in the presence of blowing. Greater increases can be expected immediately downstream of ejection with smaller increases occurring at larger distances from the cooling holes.

References

[1] Scesa, S., "Effect of Local Normal Injection on Flat-Plate Heat Transfer," Ph.D. thesis, 1954, Mechanical Engineering Dept., Univ. of California.

[2] Seban, R. A. and Back, L. H., "Effectiveness and Heat Transfer for a Turbulent Boundary Layer with Tangential Injection and Variable Free Stream Velocity," *Transactions of the ASME; Journal of Heat Transfer*, Vol. 84, Aug. 1962, pp. 235–244.

[3] Hartnett, J. P., Birkebak, R. C., and Eckert, E. R. G., "Velocity Distributions, Temperature Distributions, Effectiveness and Heat Transfer for Air Injected Through a Tangential Slot Into a Turbulent Boundary Layer," *Transactions of the ASME; Journal of Heat Transfer*, Vol. 83, Aug. 1961, pp. 293–306.

[4] Hartnett, J. P., Birkebak, R. C., and Eckert, E. R. G., "Velocity Distribution, Temperature Distributions, Effectiveness and Heat Transfer in Cooling of Surface with a Pressure Gradient," Rept. TR34, March 1961, Heat Transfer Lab., Univ. of Minnesota, Minneapolis, Minn.

[5] Metzger, D. E., Carper, H. J., and Swank, L. R., "Heat Transfer with Film Cooling Near Nontangential Injection Slots," *Journal of Engineering for Power*, April 1968.

[6] Metzger, D. E. and Fletcher, D. D., "Surface Heat Transfer Immediately Downstream of Flush Non-Tangential Injection Holes and Slots," *Journal of Aircraft*, Vol. 8, No. 1, Jan. 1971, pp. 33–38.

[7] Goldstein, R. J., Eckert, E. R. G., Eriksen, V. L., and Ramsey, J. W., "Film Cooling Following Injection Through Inclined Circular Tubes," HTL TR 91, Nov. 1969, Heat Transfer Lab., Univ. of Minnesota, Minneapolis, Minn.

[8] Carlson, L. W. and Talmor, E. "Gaseous Film Cooling at Various Degrees of Hot-Gas Acceleration and Turbulence Levels," *International Journal of Heat Mass Transfer*, Vol. 11, 1968, pp. 1695–1713.

[9] Kurosh, V. D. and Epik, E. YA., "The Effect of Turbulence on Heat Transfer in Turbomachinery Flow Passages," *Heat Transfer, Soviet Research*, Vol. 2, No. 1, Jan. 1970.

[10] Kline, S. J. and McClintock, F. A., "Describing Uncertainties in Single-Sample Experiments," *Mechanical Engineering*, Jan. 1953.